Journal of
Ceramic Science
and Technology

J. Ceram. Sci. Technol., **08** [2] 249-254 (2017)
DOI: 10.4416/JCST2016-00113
available online at: http://www.ceramic-science.com

Response Surface Methodology for Optimization of the Synthesis of Lithium Ion Conductor Glass-Ceramic Electrolyte

H. Kun*, Z. Chengkui, L. Baoying, W. Yanhang, H. Bin, C. Jiang

China Building Materials Academy, Beijing 100024 China

received November 19, 2016; received in revised form December 29, 2016; accepted February 21, 2017

Abstract

In this work, response surface methodology (RSM) based on five-level, three-variable and central composite design (CCD) was used to optimize the synthesis of Li_2O-Al_2O_3-GeO_2-P_2O_5 glass-ceramic. The effects of three independent variables, i.e. crystallization temperature, crystallization time and heating rate on the conductivity of the glass-ceramic were analyzed. The optimum conditions were found to be at the crystallization temperature of 845 °C, crystallization time of 8 h and heating rate of 3.3 K/min. In the process optimization, the highest conductivity of the glass-ceramic reached 6.3×10^{-4} S/cm, suggesting that it is a promising solid electrolyte for practical application in lithium/water batteries.

Keywords: Glass-ceramic, crystallization parameters, response surface methodology, optimization

I. Introduction

During the past few years, much attention has been paid to lithium/water secondary batteries, because they stand a good chance of achieving a better discharge capacity than conventional batteries [1,2]. Lithium/water batteries have great potential for use especially in high-discharge-capacity power supplies for long-term operation in deep-sea applications. The solid electrolyte is one of the most important components that control the properties of lithium/water secondary batteries.

In the past decades, lots of investigations have been carried out on glass-ceramic electrolyte with the general formula of $LiGe_2(PO_4)_3$, because it is particularly stable against Li metal and can be used as the solid electrolyte and the protective layer for the lithium metal electrode [11–13]. Although the conductivity of glass-ceramic is believed to be significantly affected by the chemical composition, it is not easy to fabricate a large-scale and homogeneous glass-ceramic with high Li^+ conductivity. Therefore, it is important to further investigate the parameters during the crystallization process.

Many statistical experimental design methods have been developed for process optimization in recent years [14–17]. These methods involve using mathematical models for designing chemical processes and analyzing the process results. Among them, response surface methodology stands out as a significant method utilized in many material fields [18,19].

Response Surface Methodology (RSM) has therefore been used in our research to optimize the crystallization parameters, providing factor effects and interaction effects on 3D response surfaces. The RSM method is a collection of statistical and mathematical techniques useful for developing, improving, and optimizing processes in which a response of interest is influenced by several variables and the objective is to optimize this response.

Based on our previous results [20–23], the present work was designed to assess the effects of crystallization temperature, crystallization time and heating rate on the properties of Li_2O-Al_2O_3-GeO_2-P_2O_5 glass-ceramic.

II. Experiment Procedure

(1) Synthesis and characterization

Stoichiometric amounts of Li_2CO_3, Al_2O_3, GeO_2 and $NH_4H_2PO_4$ were used as the starting materials to prepare $Li_{1.5}Al_{0.5}Ge_{1.5}(PO_4)_3$ (denoted LAGP) glass with a conventional solid solution method. The powders were weighed, mixed and milled in a high-energy milling machine for 1 h. They were then transferred to an electric furnace and heated up to 700 °C in an alumina crucible for 2 h to ensure ammonia, carbon dioxide and water vapor decompose out of the starting materials. Finally, the powders were melted at 1350 °C for 2 h and poured onto preheated stainless steel plates (~ 300 °C). The cast glass sheets measuring about 10 mm in thickness were annealed at 470 °C for 2 h to release the thermal stresses and then cooled down to room temperature. To obtain the glass-ceramic specimens, the annealed glass sheets were crystallized at 825 °C for 6 h at a heating rate of 5 K/min.

X-ray diffraction analysis, in the range from 10° to 80°, was performed by using D-max-RB diffractometer with CuKα radiation, operating at 40 kV. The microstructure of the sample was investigated by means of SEM with a field emission gun (FESEM, JSM-5510LV). The ionic conductivity was determined using impedance spectroscopy (Solartron2016 impedance analyzer) in the $0.1-10^6$ Hz frequency range, with voltage amplitude at 500 mV. After

* Corresponding author: cbmahekun@163.com

polishing, platinum was sputtered on two parallel faces of the specimen with a thickness of 1 mm in order to ensure the necessary electrical contacts. The platinum-coated specimen was assembled into a cell using a stainless steel blocking electrode in a cell fixture.

(2) Experimental design and data analysis

The Design Expert software written by STAT-EASE, INC. was employed for experimental design, data analysis and model building. Central composite design (CCD) with three variables was used to determine the response pattern and then to establish a model. Since different variables are usually expressed in different units and have different limits, the significance of their effects on response can only be compared after they are coded. For statistical calculations, the variables X_i were normalized as x_i according to the following equation:

$$x_i = \frac{X_i - X_0}{\Delta X} \quad (1)$$

where x_i is a normalized value of the variable, X_i is the actual value of the variable, X_0 is the actual value of X_i at the center point, and ΔX is the step change of the variable. In this study, the effects of three independent variables, X_1 (crystallization temperature), X_2 (crystallization time) and X_3 (heating rate), at five levels were chosen as three independent variables in the crystallization process using central composite design. The range and values of these three independent variables, presented in Table 1, were based on the results of data from preliminary experiments. The Li^+ conductivity of glass-ceramic (Y) was selected as the dependent variable. The response variable was fitted with a quadratic equation that describes the process:

$$Y = b_0 + \sum_{i=1}^{k} b_i x_i + \sum_{i=1}^{k} b_{ii} x_i^2 + \sum_{i=1}^{i \le j} b_{ij} x_i x_j \quad (2)$$

where Y represents the response, b_0 is a constant coefficient, x_i and x_j are the normalized levels for the independent variables, k is the number of independent variables, b_i, b_{ii} and b_{ij} are the coefficients for the linear, quadratic and interaction effects, respectively. The actual design of this work is presented in Table 2. The interactive effects of the independent variables on the dependent were illustrated by three-dimensional contour plots. Furthermore, the developed polynomial models were statistically validated by means of analysis of variance (ANOVA), checking their statistical significances from the F-test and their fit quality from the coefficients of determination R^2 [24–26].

Table 1: Levels of the variable tested in the 2^3 central composite design.

Variables	Range and levels				
	-1.68	-1	0	1	1.68
X_1, crystallization temperature (°C)	650	750	850	950	1050
X_2, crystallization time (h)	2	6	10	14	18
X_3, heating rate (K/min)	1	3	5	7	9

III. Results and Discussions

(1) Experiment results

The XRD pattern and FESEM micrograph of the LAGP glass-ceramic specimen are shown in Fig. 1 and Fig. 2, respectively. The NASICON-type phase of $LiGe_2(PO_4)_3$ (JCPDS card 80 – 1923) is found to be the major crystalline phase in the glass-ceramic, with minor $AlPO_4$ as the impurity crystal phase. As can be seen from Fig. 2, a homogeneous and dense structure of fine $LiGe_2(PO_4)_3$ crystals was observed in the glass-ceramic. This is the reason why the glass-ceramic fabricated under the optimal crystallization parameters exhibits the highest conductivity compared to the other specimens.

Table 2: CCD and response results for the study of three experimental variables in coded units.

No.	Coded levels			Real values			Conductivity, Y ($\times 10^{-4}$ S/cm) ±0.1 error
	x_1	x_2	x_3	X_1 (°C)	X_2 (h)	X_3 (K/min)	
1	0	0	-1.68	850	10	1	4.9
2	0	0	0	850	10	5	6.0
3	-1.68	0	0	650	10	5	5.7
4	0	0	0	850	10	1	5.8
5	0	0	0	850	10	1	5.9
6	0	-1.68	0	850	2	1	5.5
7	0	0	0	850	10	1	5.9
8	1	1	-1	950	14	3	4.8
9	1	1	1	950	14	7	5.6
10	0	1.68	0	850	18	1	5.8

No.	Coded levels			Real values			Conductivity, Y ($\times 10^{-4}$ S/cm) ±0.1 error
	x_1	x_2	x_3	X_1 (°C)	X_2 (h)	X_3 (K/min)	
11	-1	1	-1	750	14	3	5
12	-1	-1	1	750	6	7	5.3
13	-1	-1	-1	750	6	3	5.3
14	0	0	1.68	850	10	9	5.8
15	1	-1	-1	950	6	3	4.9
16	0	0	0	850	10	1	5.8
17	0	0	0	850	10	1	5.9
18	1.68	0	0	1050	10	1	5
19	-1	1	1	750	14	7	5.4
20	1	-1	1	950	6	7	5

(2) Response analysis and interpretation

It is known that RSM optimization is more advantageous than the traditional single parameter optimization because it needs fewer experiments and saves time, space and raw materials. The experimental designs and their responses are summarized in Table 2. According to the software, the final empirical models in terms of normalized factors after excluding the insignificant terms for conductivity (Y) are described in the following equation:

$$Y = 5.87513 - 0.13746X_1 - 0.137X_2 + 0.20602X_3 + 0.087500X_1X_2 + 0.062500X_1X_3 + 0.13750X_2X_3 - 0.23801X_1^2 - 0.13194X_2^2 - 0.23801X_3^2 \quad (3)$$

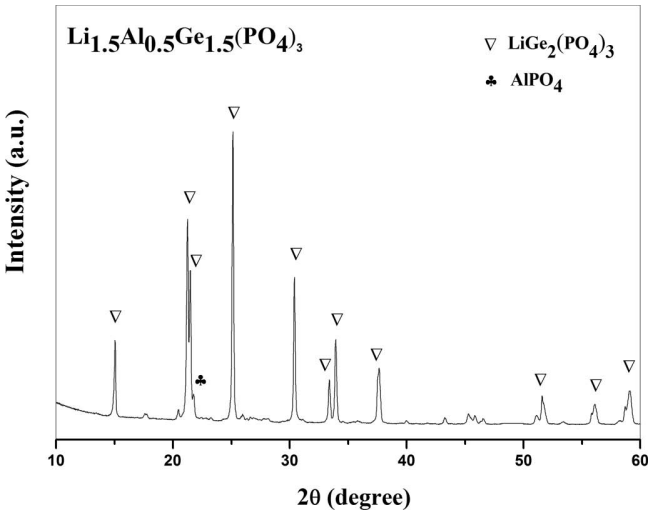

Fig. 1: XRD pattern for $Li_{1.5}Al_{0.5}Ge_{1.5}(PO_4)_3$ glass-ceramic fabricated at the optimal crystallization parameters.

Table 3 presents the ANOVA results of the quadratic model for the three dependent variables. As can be seen, the model F-value of 8.62 for conductivity (Y) implies that the model is significant. In the obtained quadratic model of the conductivity, the ratio of 7.71 indicates an adequate signal for the model to be used to navigate the design space. The F-value of the lack-of-fit of 21.75 implies it is significant relative to the pure error. There could be only 0.21 % chance that such a large p-value could occur due to noise. The normal probability plot shown in Fig. 3 indicates that the errors are normally distributed, as all the points lie very close to the line.

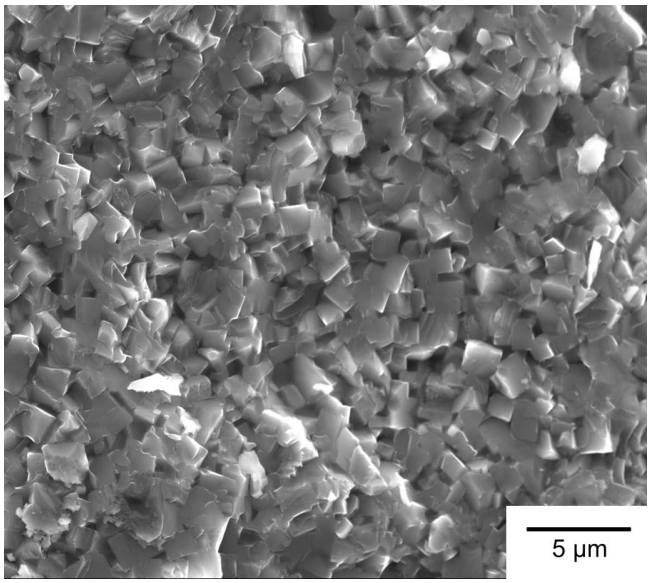

Fig. 2: Microstructure for $Li_{1.5}Al_{0.5}Ge_{1.5}(PO_4)_3$ glass-ceramic fabricated at the optimal crystallization parameters.

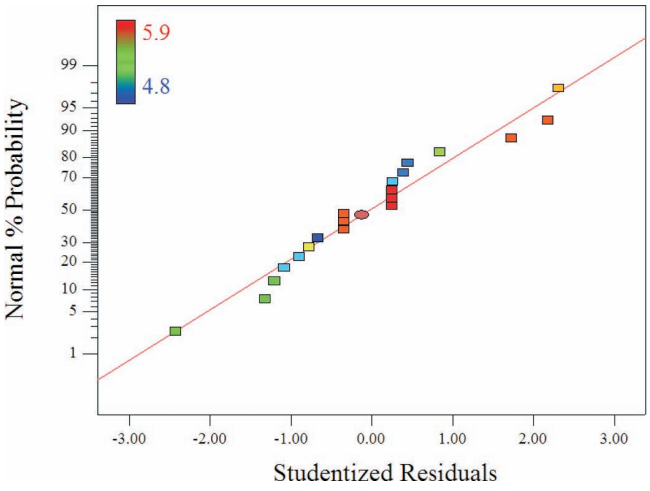

Fig. 3: Normal % probability versus studentized residuals.

Table 3: Analysis of variance (ANOVA) for response surface quadratic model for conductivity.

Source	Sum of squares	Degrees of freedom	Mean square	F value	Prob > F
Model	2.65	9	0.29	8.62	0.0012
X_1	0.26	1	0.26	7.56	0.0205
X_2	0.047	1	0.047	1.39	0.2658
X_3	0.58	1	0.580	16.99	0.0021
X_1X_2	0.061	1	0.061	1.80	0.2099
X_1X_3	0.031	1	0.031	0.92	0.3611
X_2X_3	0.15	1	0.150	4.43	0.0615
X_1^2	0.78	1	0.780	22.8	0.0008
X_2^2	0.23	1	0.230	6.73	0.0267
X_3^2	0.78	1	0.780	22.8	0.0008
Residual	0.34	10	0.034	–	–
Lack of Fit	0.33	5	0.065	21.75	0.0021

$R^2 = 0.96$, $R^2_{adj} = 0.94$, adequate precision = 7.71 (> 4)

The accuracy and variability of Equation (3) could be evaluated based on the coefficient of determination (R^2). The R^2 of the model is obtained 0.96, which indicates that 96 % of the variability in the dependent variable could be explained, and only 4 % of the total variation cannot be explained by the model [15]. The value of the adjusted determination coefficient (adj. R^2) is 0.94, which suggested that there are excellent correlations between the independent variables.

Values of Prob > F less than 0.05 indicate that the model terms are significant, whereas the values greater than 0.1000 are not significant. In this case, X_1, X_3 and the interaction terms (X_2X_3, X_1^2, X_2^2, X_3^2) are significant model terms whereas X_2 and the interaction terms (X_1X_2, X_1X_3) are insignificant to the response. From the statistical results obtained, it is shown that the above model was adequate to predict the conductivity of LAGP glass-ceramic within the reasonable range of the variables studied.

The predicted values of conductivity for LAGP glass-ceramic were calculated with Equation (3) and compared with experimental values in Fig. 4. The clustering of the points around the diagonal line indicates a satisfactory correlation between the experimental and predicted values, thereby confirming the soundness of the model.

(3) Interactions among the factors

With consideration of two variables at one time while keeping the third variable at the middle level, the three-dimensional response surface plots and two-dimensional contour plots of LAGP glass-ceramic were constructed according to Equation (3). Fig. 5 shows the effect of crystallization temperature and time on the conductivity of LAGP glass-ceramic at a fixed heating rate of 5 K/min. It can be seen from Fig. 5 that the conductivity of the LAGP glass-ceramic increased with the crystallization temperature from 650 °C to 850 °C and then decreased from 850 °C to 1050 °C. The crystallization time had a significant effect on the conductivity, which increased from 2 to 10 h and decreased from 10 to 18 h.

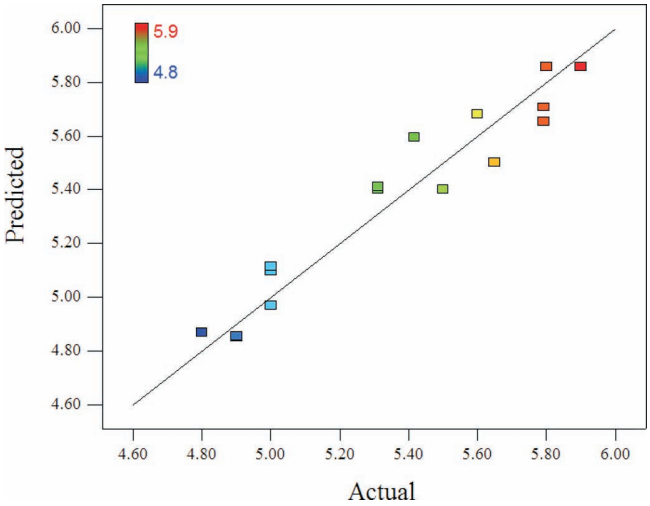

Fig. 4: Linear correlation between observed and predicted values.

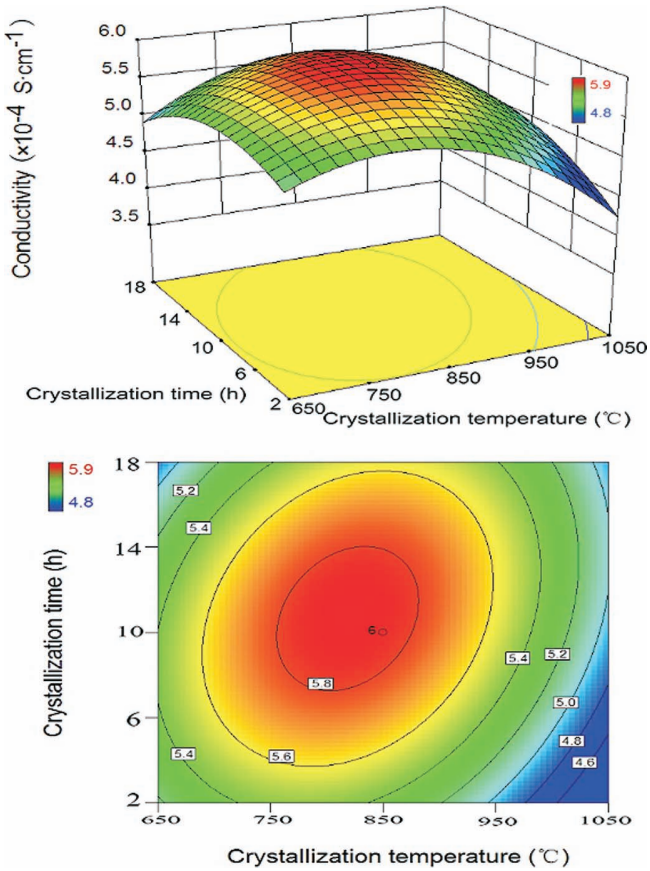

Fig. 5: The 3D response surface and 2D contour plots of crystallization temperature vs. crystallization time on conductivity at center level of heating rate.

A similar phenomenon could be found from the effect of the crystallization temperature and heating rate on the conductivity of the LAGP glass-ceramic in Fig. 6. As can be seen, the conductivity of the LAGP glass-ceramic increased with heating rate from 1 to 5 K/min, and decreased with an increase in the heating rate from 5 to 9 K/min. As

shown in Fig. 6, the highest conductivity of 6.0×10^{-4} S/cm was observed at a heating rate of 5 K/min and crystallization temperature of 850 °C.

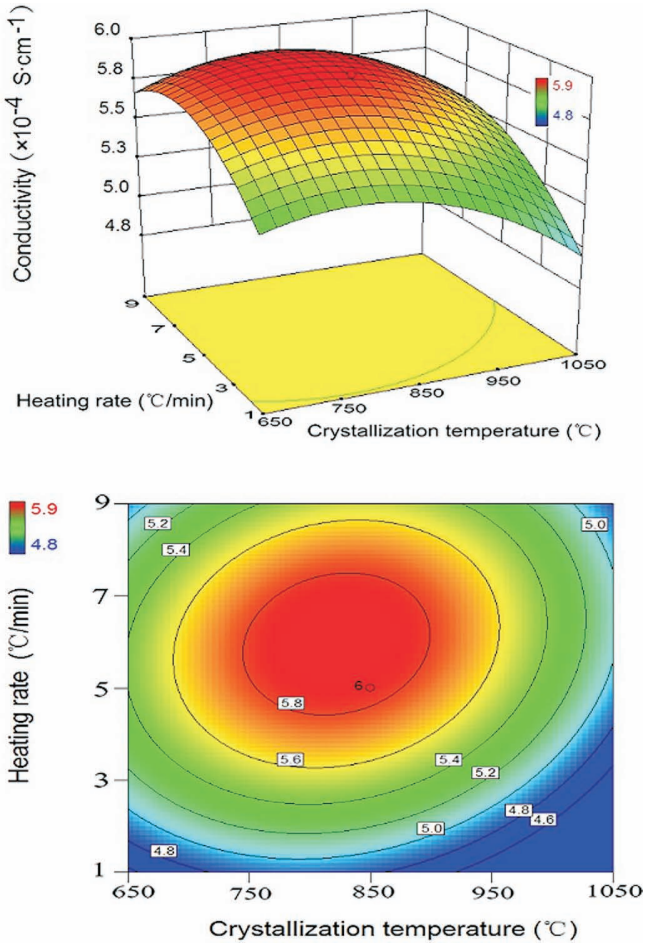

Fig. 6: The 3D response surface and 2D contour plots of crystallization temperature vs. heating rate on conductivity at center level of crystallization time.

Fig. 7 shows the effect of the crystallization time and heating rate on the conductivity of the LAGP glass-ceramic that crystallized at 850 °C. Increasing the crystallization time from 2 to 18 h led to a rise in the glass-ceramic conductivity when the heating rate changed from 1 to 4 K/min. However, the conductivity of the glass-ceramic increased slightly and then decreased when the heating rate changed from 5 to 9 K/min. On reduction of the heating rate, a similar phenomenon was observed for the conductivity of the glass-ceramic in condition of high crystallization time (10 to 18 h) and low crystallization time (2 to 10 h), respectively.

(4) Process optimization and microstructures of the glass-ceramic

An optimization study was carried out to evaluate the optimal crystallization parameters for LAGP glass-ceramic with high Li^+ conductivity. Table 4 shows the optimum crystallization parameters based on combination of all the 3D response surfaces and 2D contour plots. These optimal crystallization parameters were found to be at the temperature of 845 °C, time of 8 h and heating rate of 3.3 K/min. The estimated Li^+ conductivity of the LAGP glass-ceramic was 6.0×10^{-4} S/cm while the experimental value was 5.9×10^{-4} S/cm. Only a small deviation (1.67 %) was found between the experimental value and the predicted value. Therefore, the central composite design (CCD) design can be used to optimize the crystallization process of LAGP glass-ceramic.

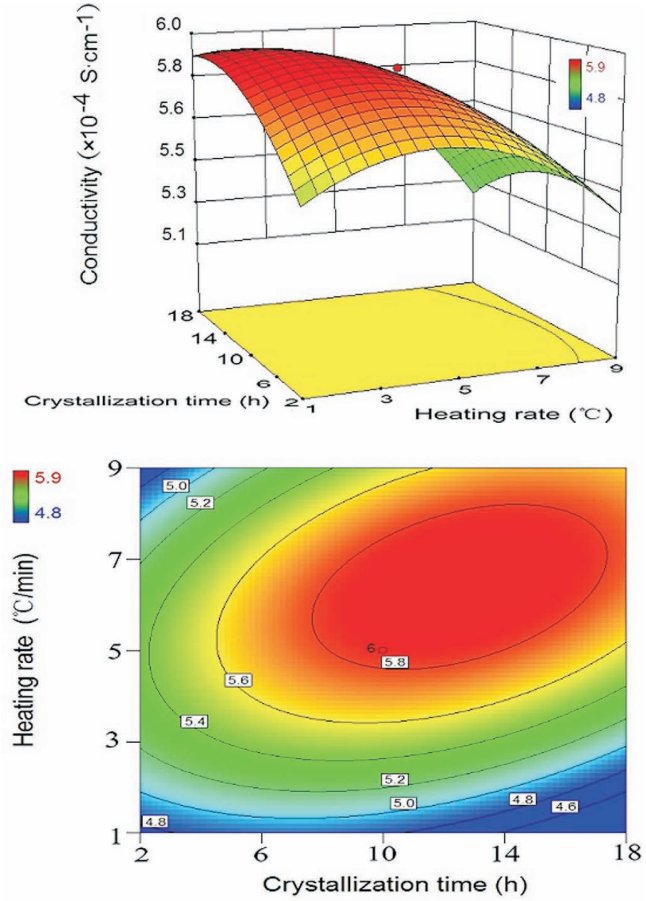

Fig. 7: The 3D response surface and 2D contour plots of crystallization time vs. heating rate on conductivity at center level of crystallization temperature.

Table 4: The predicted and experimental values of the responses at optimal conditions.

Crystallization temperature (°C)	Crystallization time (h)	Heating rate (K/min)	Li^+ conductivity ($\times10^{-4}$ S/cm)	
			Predicted value	Experimental value
845	8	3.3	6.0	5.9

IV. Conclusions

This research was carried out to determine the optimal crystallization parameters for Li_2O-Al_2O_3-GeO_2-P_2O_5 glass-ceramic. The quadratic term of the crystallization temperature multiplier, heating rate, and the interaction between crystallization time and heating rate are insignificant factors. According to the obtained quadratic model for Li^+ conductivity, the optimal crystallization parameters were found to be at the temperature of 845 °C, crystallization time of 8 h and heating rate of 3.3 K/min. Furthermore, the deviation was found to be 1.67 % between

the experimental values and the predicted values, indicating that the CCD design can be used to optimize the crystallization process of LAGP glass-ceramic.

References

1 Armand, M., Tarascon J.M.: Building better batteries, *Nature*, **451**, 652 – 657, (2008).

2 Feng, J.K., Lu, L., Lai, M.O.: Lithium storage capability of lithium ion conductor $Li_{1.5}Al_{0.5}Ge_{1.5}(PO_4)_3$, *J. Alloy. Compd.*, **501**, 255 – 258, (2010).

3 Aono, H., Sugimoto, E., Sadaoka, Y., Imanaka, N., Adachi, G.: Ionic conductivity of the lithium titanium phosphate systems ($Li_{1+x}M_xTi_{2-x}(PO_4)_3$, M= Al, Sc, Y and La), *J. Electrochem. Soc.*, **136**, 590 – 591, (1989).

4 Leo, C.J, Chowdari, B.V.R, Rao, G.V.S.: Lithium conducting glass ceramic with NASICON structure, *Mater. Res. Bull.*, **37**, 1419 – 1430, (2002).

5 Xu, X.X., Wen, Z.Y., Gu, Z.H.: Preparation and characterization of lithium ion-conducting glass ceramics in the $Li_{1+x}Cr_xGe_{2-x}(PO_4)_3$ system, *J. Am. Ceram. Soc.* **90**, 2802 – 2808, (2007).

6 Fu, J.: Fast Li^+ ion conducting glass ceramics in the system Li_2O-Al_2O_3-GeO_2-P_2O_5, *Solid State Ionics*, **104**, 191 – 194, (1997).

7 Thokchom, J.S., Gupta, N., Kumar, B: Superionic conductivity in a lithium aluminum germanium phosphate glass-ceramic, *J. Electrochem. Soc.*, **155**, 915 – 920, (2008).

8 Mariappan, C.R., Yada, C., Rosciano, F., Roling, B.: Correlation between micro-structural properties and ionic conductivity of $Li_{1.5}Al_{0.5}Ge_{1.5}(PO_4)_3$ ceramics, *J. Power Sources,* **196**, 6456 – 6464, (2011).

9 Cruz, A.M., Ferreira, E.B., Rodrigues, A.C.M.: Controlled crystallization and ionic conductivity of a nanostructured $LiAlGePO_4$ glass-ceramic, *J. Non-Cryst. Solids*, **35**, 2295 – 2301, (2009).

10 Xu X.X., Wen, Z.Y., Wu, X., Gu, Z.H.: Preparation and characterization of lithium ion-conducting glass ceramics in the $Li_{1+x}Cr_xGe_{2-x}(PO_4)_3$ system, *J. Am. Ceram. Soc.*, **90**, 2802 – 2808, (2007).

11 Fernandez, C., Verné, E., Vogel, J., Carl, G.: Optimisation of the synthesis of glass-ceramic matrix biocomposites by the response surface methodology, *J. Eur. Ceram. Soc.,* **23**, 1031 – 1038, (2003).

12 Aslan, N.: Application of response surface methodology and central composite rotatable design for modeling and optimization of a multi-gravity separator for chromite concentration, *Powder Technol.*, **185**, 80 – 86, (2008).

13 Li, G.L, Zhang, X.L., You, J.M.: Highly sensitive and selective pre-column derivatization high-performance liquid chromatography approach for rapid determination of triterpenes oleanolic and ursolic acids and application to swertia species: optimization of triterpenic acids extraction and pre-column derivatization using response surface methodology, *Anal. Chim. Acta*, **688**, 208 – 218, (2011).

14 Chen, G., Peng, J.H., Chen, J.: Optimizing conditions for wet grinding of synthetic rutile using response surface methodology, *Miner. Metall. Process.*, **28**, 44 – 48, (2011).

15 Chen, G., Chen, J., Srinivasakannan, C., Peng J.H.: Application of response surface methodology for optimization of the synthesis of synthetic rutile from titania slag, *Appl. Surf. Sci.*, **258**, 3068 – 3073, (2012).

16 Nassar, A.I., Thom, N., Parry, T.: Optimizing the mix design of cold bitumen emulsion mixtures using response surface methodology, *Constr. Build. Mater.*, **104**, 216 – 229, (2016).

17 Qin, X.P., Wang, Y.L., Lu, C.H., *et al.*: Structural acoustics analysis and optimization of an enclosed box-damped structure based on response surface methodology, *Mater. Design*, **103**, 236 – 243, (2016).

18 Zhang, X.Y., Liu, J.P., Qiao, H., Liu, H., Ni, J.M., Zhang, W.L., Shi, Y.B.: Formulation optimization of dihydroartemisinin nanostructured lipid carrier using response surface methodology, *Powder Technol.*, **197**, 120 – 128, (2010).

19 Chen, G., Peng, J.H., Chen, J., Zhang, S.M.: Response surface methodology applied to optimize the experimental conditions for preparing synthetic rutile by microwave irradiation, *High Temp. Mater. Proc.*, 28, 165 – 168, (2009).

20 He, K., Wang, Y.H., Zu, C.K., *et al.*: Influence of Al_2O_3 additions on crystallization mechanism and conductivity of Li_2O-Al_2O_3-GeO_2-P_2O_5 glass-ceramics, *Physica B*, **06**, 3947 – 3950, (2014).

21 He, K., Wang, Y.H., Zu, C.K., *et al.*: Crystallization kinetics of lithium aluminum germanium phosphate glass by DSC technique, *J. Wuhan Univ. Technol.,* **27**, 63 – 66, (2012).

22 He, K., Wang. Y.H, Zu, C.K., *et al.*: High-temperature x-ray analysis of phase evolution in lithium ion conductor $Li_{1.5}Al_{0.5}Ge_{1.5}(PO_4)_3$, *Mater. Charact.*, **80**, 86 – 91, (2013).

23 He, K., Wang, Y.H., Zu, C.K., *et al.*: Stability of lithium ion conductor NASICON structure glass ceramic in acid and alkaline aqueous solution, *Solid State Ionics*, **254**, 78 – 81, (2014).

24 Wang, J.P., Chen, Y.Z., Ge, X.W., Yu, H.Q.: Optimization of coagulation-flocculation process for a paper-recycling wastewater treatment using response surface methodology, *Colloid. Surface. A*, **302**, 204 – 210, (2007).

25 Li, Y., Cui, F., Liu, Z., Xu, Y., Zhao, H.: Improvement of xylanase production by penicillium oxalicum ZH-30 using response surface methodology, *Enzyme Microb. Tech.*, **40**, 1381 – 1388, (2007).

26 Hashemi, M., Razavi, S.H., Shojaosadati, S.A., Mousavi, S.M., Khajeh, K., Safari M.: Development of a solid-state fermentation process for production of an alpha amylase with potentially interesting properties, *J. Biosci. Bioeng.*, **110**, 333 – 337, (2010).